PERGAMON

International Journal of Solids and Structures 37 (2000) 6981–7001

INTERNATIONAL JOURNAL OF SOLIDS and STRUCTURES

www.elsevier.com/locate/ijsolstr

# A numerical continuation method based on Padé approximants

Ahmad Elhage-Hussein [a], Michel Potier-Ferry [a], Noureddine Damil [b,*]

[a] *Laboratoire de Physique et Mécanique des Matériaux, UMR CNRS 7554, Institut Supérieur de Génie Mécanique et Productique, Université de Metz, Ile du Saulcy, 57045 Metz cedex 01, France*

[b] *Laboratoire de Calcul Scientifique en Mécanique, Faculté des Sciences Ben M'Sik, Université Hassan II, Sidi Othman, Casablanca 7955, Morocco*

Received 10 November 1999

**Abstract**

A continuation algorithm is presented with a new predictor, which is based on a rational representation of the solution path. This algorithm belongs to the class of asymptotic numerical methods that connect perturbation techniques with a discretization principle without the use of a correction process. Several examples from shell buckling and from contact mechanics are analyzed, to assess the efficiency and the reliability of the method. 

*Keywords:* Asymptotic numerical methods; Perturbation technique; Padé approximants; Contact; Buckling; Elastic shells

## 1. Introduction

In this article, we present a new algorithm for the numerical computation of a solution path $\mathbf{u}(\lambda)$, where $\mathbf{u}$ is the unknown and $\lambda$ is a scalar parameter. Classically, this type of problem is computed by using iterative predictor–corrector methods. The present algorithm belongs to the class of asymptotic numerical methods (ANM), that associate a perturbation technique with a discretization principle. Within this framework, the solution path is represented by truncated power series in the form:

$$\begin{cases} \mathbf{S}_n(\mathbf{u}(a)) = \mathbf{u}_0 + a\mathbf{u}_1 + \cdots + a^n\mathbf{u}_n, \\ S_n(\lambda(a)) = \lambda_0 + a\lambda_1 + \cdots + a^n\lambda_n, \end{cases} \tag{1}$$

where $a$ is a suitable path parameter. Such ideas were introduced a long time ago, see for instance, Thompson and Walker (1968), Kawahara et al. (1976) and Noor and Peters (1981).

The range of validity of representation (1) is slightly smaller than the radius of convergence of the series. As this radius is generally finite, a given solution path must be computed with a step-by-step method. In

* Corresponding author. Tel.: +212-2-704671/72/73; fax: +212-2-704675.

*E-mail addresses:* elhage@lpmm.univ-metz.fr (A. Elhage-Hussein), potier-ferry@lpmm.univ-metz.fr (M. Potier-Ferry), ciu@techno.net.ma (N. Damil).

0020-7683/00/$ - see front matter 
PII: S0020-7683(99)00323-6

most of the cases, within ANM, the new starting point is the last point of the previous step. A very simple criterion has been introduced by Cochelin (1994), that gives a closed-form expression for the last point. This criterion has been successfully applied in many fields: classical elastic shells (Cochelin et al., 1994a), plastic beams (Braikat et al., 1997), elastic shell models allowing large rotations (Zahrouni et al., 1999), elastic plastic shells (Zahrouni et al., 1998; Zahrouni, 1998), Navier–Stokes equations (Tri et al., 1996; Cadou et al., 1998), Norton-Hoff materials (Potier-Ferry et al., 1997; Potier-Ferry et al., 1998), contact mechanics (Elhage-Hussein et al., 1998). The plastic model considered so far remained restricted to the deformation theory. That algorithm is very robust when the response curve has sudden slope changes, especially when this is due to quasi-bifurcations (Cochelin et al., 1994a; Tri et al., 1996; Vannucci et al., 1998; Zahrouni et al., 1998) or due to contact with a rigid obstacle (Elhage-Hussein et al., 1998). This reliability in path following calculations is probably the main advantage of ANM with respect to iterative algorithms. Only occasionally, a correction phase is necessary to define the new starting point, for instance to obtain a very high accuracy to be able to detect bifurcation points (Vannucci et al., 1998). Thus up to now, the ANM has been applied in such a way that it appears as a continuation method without any corrector iteration or with sporadic corrector iterations: the only exception seems due to Brunelot (1999) and Potier-Ferry et al. (1998) in the case of viscoplastic bodies. Another criterion similar to (9) can be used, that is based on the residual vector, but it is practically as effective as the criterion (9), see Zahrouni et al. (1999).

Many detailed studies have been presented in the literature to compare the computation time and the number of matrix decompositions necessary for a given solution path by the continuation method based on formula (1) or by more classical approaches. It is not an easy matter to choose the 'best' classical method for a given problem. The modified Newton method is efficient when it works, but it is generally rejected for lack of reliability. The Newton–Raphson method with a prescribed step length has not the same drawback, but it yields much greater computation times than the ANM, at least for large scale problems, i.e. when the number of degrees of freedom is beyond 2000: this is not surprising, because the step lengths of ANM are naturally adaptative, what is a great advantage (Ammar, 1996; Brunelot, 1999; Cadou et al., 1998). The best reference should be the Newton–Raphson method with an adaptative step length, but there are many possible computational strategies. Different comparisons have been achieved between ANM and such iterative algorithms proposed by industrial codes: ones again, the ANM has been the most efficient, sometimes with significant differences (Elhage-Hussein et al., 1998; Elhage-Hussein, 1998; Zahrouni et al., 1999, 1998). Thus, the ANM seems at least as efficient as incremental-iterative algorithms and this point will not systematically be rediscussed in this article.

Here, the aim is to improve the continuation method based on formula (1), by replacing the polynomial approximation (1) by a rational one as follows:

$$\begin{aligned} \mathbf{P}_n(\mathbf{u}(a)) &= \mathbf{u}_0 + \sum_{k=1}^{n} f_k(a)\mathbf{u}_k, \\ f_k(a) &= P_k(a)/Q_k(a), \end{aligned} \tag{2}$$

where $P_k$ and $Q_k$ are polynomials. Well-established techniques exist to replace a polynomial representation such as (1) by a rational one. The corresponding functions are called Padé approximants (Padé, 1892; Van-Dyke, 1984; Baker and Morris, 1996). Padé approximants have first been applied for the numerical solution of continuous problems by Azrar et al. (1992) and many tests have been carried out in various fields to verify its effectiveness (Boutyour et al., 1993; Cochelin et al., 1994b; de Boer and van Keulen, 1997; Tri et al., 1996; Braikat et al., 1997). In any case, the rational approximation has a greater range of validity than the polynomial one. Unfortunately a rational fraction such as (2) has poles, which is generally not in accordance with the exact solution. To define a reliable continuation method, one has to detect these undesirable poles and to eliminate them from the range of validity of the approximation, what is one of the main difficulties to define a proper continuation method.

Another variant is the reduced basis technique, which uses the computed vectors $\mathbf{u}_i$ as a basis in a Rayleigh–Ritz approximation (Almroth et al., 1978; Noor, 1981; Noor and Peters, 1980, 1981; Lewandowski, 1987). This seems very attractive, firstly, because there are other ways to build up a basis so that one is not restricted to the one deduced from the perturbation technique and secondly, because it yields a priori a larger step length than the series or the rational approximation. A detailed comparison has been made between representations (1) and (2) and the reduced basis technique (Najah et al., 1998). In this article, it was shown that the step lengths obtained by the rational approximation are close to those of the reduced basis technique, but that the computational cost to obtain the reduced system increases drastically with the order $n$, which limits the applications of the latter method to small orders. According to these authors, the reduced basis technique is not the most efficient as long as a fast algorithm to compute the reduced system is not found. That is why we focus here on the rational approximation (2).

This article is organized as follows. In Section 2, we review the basic asymptotic numerical algorithms: computation of the series, the continuation technique and Padé Approximants. The only new feature is here a technique to evaluate the radius of convergence, which permits a redefinition of the range of validity of the two approximations (1) and (2) and that shows why the simple criterion (9) can be used as an estimate of this range of validity. Next in Section 3, a continuation procedure associated with the rational approximation (2) is presented and validated. Finally, in Section 4, several classical examples related to shell buckling and contact mechanics are analyzed by this new continuation method to assess its efficiency and reliability.

## 2. A review of the asymptotic numerical methods

### 2.1. Generalities

We are interested in the numerical computation of a solution path $\mathbf{U}(\lambda)$ of a non-linear problem in the following form:

$$L(\mathbf{U}) + Q(\mathbf{U},\mathbf{U}) = \lambda \mathbf{F}, \tag{3}$$

where $\mathbf{U}$ is the unknown, $\lambda$, a scalar parameter, $L$, a linear operator, $Q$, a non-linear quadratic operator and $\mathbf{F}$, a given vector. Navier–Stokes equations are naturally written in that framework (Cadou et al., 1998), but also the governing equations of geometrically non-linear elasticity (Cochelin et al., 1994a) provided that the unknown $\mathbf{U} = (\mathbf{u}, \mathbf{S})$ includes the displacement field $\mathbf{u}$ and the second Piola–Kirchhoff stress tensor $\mathbf{S}$. In this article, we confine ourselves to applications in non-linear elasticity with or without contact conditions. At this level, the discretization process is not begun and Eq. (3) is a set of partial differential equations and of boundary conditions.

The basic idea of the asymptotic numerical method is to search a parametric representation of the solution path $(\mathbf{U}(a), \lambda(a)) = (\mathbf{u}(a), \mathbf{S}(a), \lambda(a))$ in the form of integro-power series (1), in the neighborhood of an initial solution $(\mathbf{U}_0, \lambda_0)$ with respect to an appropriately chosen parameter $a$. The vector fields $\mathbf{U}_n = (\mathbf{u}_n, \mathbf{S}_n)$ are solutions of a recurrent sequence of linear problems, with a single tangent operator. Afterwards, the stress field $\mathbf{S}_n$ obtained by the perturbation technique is substituted into the corresponding equilibrium equations and this condensation of the stress leads to partial differential equations for $\mathbf{u}_n$ that are next discretized by the finite element method. The details of the algorithm have been published several times and are not repeated here (Cochelin et al., 1994a; Elhage-Hussein et al., 1998). Note that the order of the sequence perturbation-condensation-discretization is not compulsory, but it is important to compute separately and to store all the stress fields $\mathbf{S}_n$. Problems involving contact (Elhage-Hussein, 1998; Elhage-Hussein et al., 1998) can also be put in such a framework by adding a contact potential energy function. The governing equations are then written as follows:

$$L(\mathbf{U}) + Q(\mathbf{U},\mathbf{U}) = \lambda \mathbf{F} + \mathbf{R}(\mathbf{u}),$$

where **R** is the contact force vector at the contact points, which can be defined as a function of displacement via a regularized contact law (Elhage-Hussein et al., 1998). The range of validity of the representation (1) depends strongly on the path parameter $a$. But the natural choice $a = \lambda$, that is often made in the literature, is not the best one (Cochelin et al., 1994b). In the ANM, one usually defines the path parameter $a$ as a quasi-arc-length parameter:

$$a = \langle \mathbf{u} - \mathbf{u}_0, \mathbf{u}_1 \rangle + (\lambda - \lambda_0)\lambda_1. \tag{4}$$

It is possible to improve the range of validity by replacing the polynomial approximation (1) by a rational one called Padé approximants (Baker and Morris, 1996; Brezinski and Iseghem, 1994; Cochelin et al., 1994b). But because the representation (1) is not a scalar series, we introduce, see Cochelin et al. (1994b), an ortho-normal basis $\mathbf{u}_i^*$ from the vectors $\mathbf{u}_i$ by a classical Gram–Schmidt orthogonalization procedure:

$$\mathbf{u}_i = \sum_{j=1}^{i} \alpha_{ij} \mathbf{u}_j^*, \quad i = 1, n. \tag{5}$$

Introducing Eq. (5) in the polynomial representation (1), we obtain $n$ polynomials with decreasing degrees as factors of the vector fields $\mathbf{u}_k^*$.

$$\mathbf{u} - \mathbf{u}_0 = \sum_{i=1}^{n} a^i \mathbf{u}_i^* \left( \sum_{j=i}^{n} \alpha_{ji} a^{j-i} \right).$$

In the next step, this new representation is truncated at an order about $n/2$ and each polynomial is replaced by a suitable rational fraction. These rational approximants sometimes present the disadvantage to have a number of poles close to the radius of convergence. To avoid this drawback, we proposed in Najah et al. (1998) an alternative way to replace the polynomials by rational fractions with a single denominator (see Appendix A). These fractions are called simultaneous Padé approximants or vector Padé approximants (Baker and Morris, 1996; Brezinski and Iseghem, 1994). Finally, we arrive at a new representation by a rational fractions of the solution path $\mathbf{u}(\lambda)$ in the form,

$$\begin{cases} \mathbf{P}_n(\mathbf{u}(a)) = \mathbf{u}_0 + a\frac{D_{n-2}}{D_{n-1}}\mathbf{u}_1 + \cdots + a^{n-1}\frac{1}{D_{n-1}}\mathbf{u}_{n-1}, \\ P_n(\lambda(a)) = \lambda_0 + a\frac{D_{n-2}}{D_{n-1}}\lambda_1 + \cdots + a^{n-1}\frac{1}{D_{n-1}}\lambda_{n-1}, \end{cases} \tag{6}$$

where $D_i(a)$ are polynomials of degree $(i)$ with real coefficients $(d_i)_{[i=1,n-1]}$:

$$D_i(a) = 1 + ad_1 + a^2 d_2 + \cdots + a^i d_i. \tag{7}$$

Those rational fractions have been tested in many cases (Braikat et al., 1997; Najah et al., 1998). The Padé approximants seem to increase significantly the range of validity of the polynomial representation. The aim of this article is to establish a robust continuation method with rational representation, as it has been done with the polynomial approximation.

In what follows, we shall use several definitions for the end of step. First, $a_{\mathrm{rc}}$ will be the radius of convergence of the infinite series. By $a_{\mathrm{LS}}$, we designate the theoretical limit of validity of the truncated series (1) in order that the residual remains lower than a given value, and $a_{\mathrm{LP}}$ will be the equivalent for the Padé approximation (2). Last, we define other limits of validity $a_{\mathrm{ms}}$ and $a_{\mathrm{mp}}$ that will be practically used in the continuation process.

### 2.2. Estimation of the radius of convergence

In this section, we introduce a method to compute the denominator's roots of the fractions (6) with the aim to estimate the radius of convergence. Indeed, it is known that the first pole of a Padé approximant may

be considered as a good approximation of the radius of convergence of the corresponding series (Baker and Morris, 1996). For this reason, we calculate, using a Bairstow algorithm (see Appendix B), all the complex and real roots of the denominator (7) for $i = n - 1$. But in the sequel, we shall present only the root which admits the smallest modulus. The main point of this section is to examine if the poles can give a good estimate of the radius of convergence, denoted by $a_{rc}$.

### 2.2.1. Cylindrical shell under axial loading

The first test concerns a cylindrical shell with two diametrically opposed rectangular cutouts, which are placed in the middle. The characteristics of the shell are given in Fig. 1. It is subjected to a uniform axial compression $\lambda P$, $P = 981$ N/mm. Due to the symmetry, only one octant of the structure is considered in this analysis. The structure is discretized using three nodes DKT shell elements, with a mesh involving 5190 degrees of freedom.

The response curve load–deflection in the middle of the cutout, given in Fig. 1, has been obtained by a continuation method. It is compared with a one step ANM solution. This step has been computed at orders 5, 10 (Fig. 1).

In Table 1, the variation of the first real and complex poles of Padé approximants are given in dependence of the truncation order of the series.

In this example, we remark that the dominant poles are complex and that their moduli are very small, as compared with the real ones. The real poles depend on the order and are not representative of the studied response curve. On the contrary, the first complex pole varies more regularly and seems to converge to a limit value $a_{rc} = 14.1$, when the order of truncation increases. So, it is consistent to conclude that the radius of convergence is equal to 14.1. In addition, we notice that, by calculating only 20 terms of the series, we can estimate this radius with an error of about 1%.

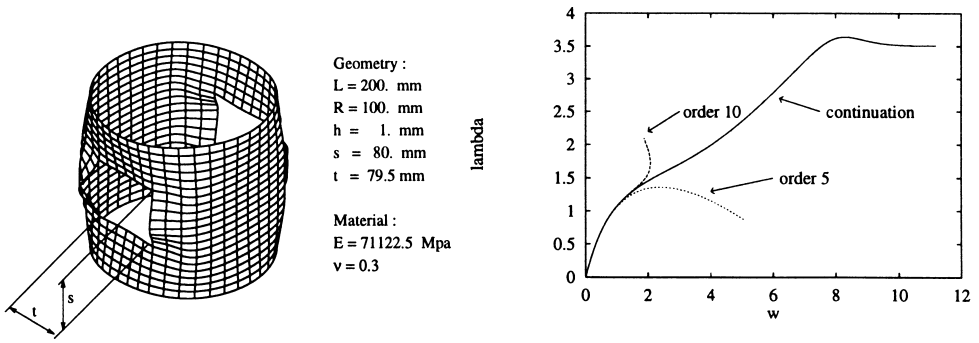


Fig. 1. Cylindrical shell under axial loading. Loading parameter/radial displacement.

Table 1
Cylinder: the first real and complex poles

| Order | First complex pole modulus | First real pole |
|---|---|---|
| 5 | 21.0638 | 9658.1498 |
| 10 | 15.3256 | 11369.835 |
| 15 | 14.4187 | 3147.8524 |
| 20 | 14.2465 | 153.3270 |
| 25 | 14.1798 | 48901.4020 |
| 30 | 14.1382 | 85.6769 |
| 35 | 14.1043 | 83.6912 |

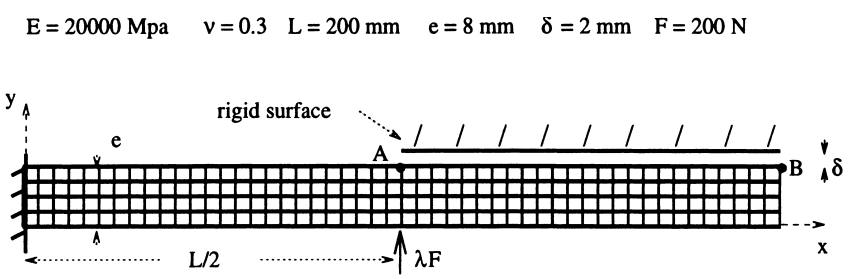


Fig. 2. Contact between an elastic beam and a rigid segment.

*2.2.2. Contact between an elastic beam and a plane rigid surface*

We consider the contact problem between an elastic beam and a plane rigid surface (Fig. 2). This contact problem has been solved by the ANM and we refer to Elhage-Hussein et al. (1998) and Elhage-Hussein (1998) for details about the contact algorithm. The line AB contains 26 contact nodes. The structure is discretized by 4-node quadrilateral elements with a mesh involving 510 degrees of freedom. The contact force $R$ at each contact node is regularized by the hyperbolic equation $R = \eta(\delta - h)/h$, where $h$ is the clearance, $\delta$ is the initial clearance, and $\eta$ is a small regularization parameter. In this test, we have chose $\eta = 10^{-4}$.

This contact definition admits a singular point at $h = 0$. So, one can expect that this singularity will lead to a real pole when we use Padé approximants.

In Table 2, we present the first real and complex poles with the corresponding truncation orders.

For this example, the dominant poles are real. We can also see, as in the case of the cylinder, the first real pole converges to a limit value $a_{rc} = 17.06$ that we adopt as the radius of convergence.

As in the previous example, the first pole with truncation at an order 20 seems to give a good estimate of the radius of convergence of the series.

*2.3. Range of validity of the asymptotic numerical methods representations*

In the numerical solution, we do not compute the series, but the truncated series (1) or the rational approximation (2). So, we have to define a range of validity of these two approximations, that will be noted respectively $a_{LS}$ and $a_{LP}$. These validity limits depend on the truncation order and on the required accuracy. In this section, the series will be truncated at an order 20 and the solution is supposed to be acceptable if the residual norm is smaller than $10^{-3}$.

The evolution of the residual vector along the computed response curves is presented in Appendix C, for the two previously presented problems.

According to this criterion, the polynomial solution of the cylinder problem is acceptable until a limit value $a_{LS} = 10.7817$ ($a_{LS}/a_{rc} = 0.7644$) of the parameter $a$, which is then clearly inside the radius of con-

Table 2
Contact: the first real and complex poles

| Order | First complex pole modulus | First real pole |
|---|---|---|
| 5 | – | 18.8129 |
| 10 | – | 17.2527 |
| 15 | 4494.9680 | 17.0831 |
| 20 | 23.4521 | 17.0491 |
| 25 | 18.8882 | 17.0578 |
| 30 | 17.7219 | 17.0584 |
| 35 | 17.2077 | 17.0619 |

Table 3
Cylinder: evaluation of $a_{ms}$

| Order | | 10 | 15 | 20 | 25 | 30 |
|---|---|---|---|---|---|---|
| $\epsilon = 10^{-7}$ | $a_{ms}$ | 3.7949 | 6.1656 | 7.7396 | 8.8359 | 9.6426 |
| | $\log_{10}$(residual) | −6.3220 | −6.1337 | −6.0250 | −5.9009 | −5.7642 |
| $\epsilon = 10^{-5}$ | $a_{ms}$ | 6.3302 | 8.5670 | 9.8624 | 10.7049 | 11.3021 |
| | $\log_{10}$(residual) | −4.0386 | −3.9337 | −3.8567 | −3.7511 | −3.6352 |
| $\epsilon = 10^{-3}$ | $a_{ms}$ | 10.5594 | 11.9039 | 12.5673 | 12.9693 | 13.2473 |
| | $\log_{10}$(residual) | −1.7231 | −1.7190 | −1.6766 | −1.5960 | −1.5078 |

vergence (Appendix C, Table 1). Concerning the rational solution, the limit of validity is equal to $a_{LP} = 16.0179$ ($a_{LP}/a_{rc} = 1.1357$) and it is greater than the radius of convergence, given in Section 2.2 (Appendix C, Table 2).

With the contact problem, the solution is acceptable until contact at node B takes place, which corresponds to the value $a_{LS} = 15.6564$ ($a_{LS}/a_{rc} = 0.9176$) of the control parameter (Appendix C, Table 3).

For the two examples, the limits of validity of the series are slightly smaller than the radii of convergence, in agreement with the series theory.

### 2.4. Continuation method based on the series

Because of this limit of validity, the solution path has to be defined step by step. Generally within ANM, the end of step criterion and the continuation method are not based on the calculation of the residual, for two reasons: First, one tries to avoid the computation of many residual vectors. Second, the residual tends to increase along the path so that a correction phase would be necessary at each end of step to correctly initiate the residual for the next step. To avoid a second matrix inversion per step, one tries to shorten the step and to have a smaller residual at the end of step (say $10^{-5}$–$10^{-4}$), which permits to choose the new starting point at the end of the last step: according to the results given in Appendix C, the step shortening due to this strategy is rather small. Cochelin has proposed in (Cochelin, 1994) a simple criterion, by requiring that the difference between two successive orders must be smaller than a given accuracy parameter $\epsilon$:

$$\frac{\|\mathbf{S}_n - \mathbf{S}_{n-1}\|}{\|\mathbf{S}_n - \mathbf{u}_0\|} = \frac{\|a^n \mathbf{u}_n\|}{\|a\mathbf{u}_1 + \cdots + a^n \mathbf{u}_n\|} < \epsilon. \tag{8}$$

If one approximates the denominator by the first term, the maximal value is then given by a closed-form expression for the maximal value $a_{ms}$:

$$a_{ms} = \left(\epsilon \frac{\|\mathbf{u}_1\|}{\|\mathbf{u}_n\|}\right)^{1/(n-1)}. \tag{9}$$

Such an analysis has been carried out by Cochelin (1994) and various tests have shown that the path following procedure so-defined is efficient and reliable (Ammar, 1996; Braikat et al., 1997; Cochelin et al., 1994a; Cadou et al., 1998; Elhage-Hussein et al., 1998; Potier-Ferry et al., 1997; Tri et al., 1996; Vannucci et al., 1998; Zahrouni, 1998; Zahrouni et al., 1999; Zahrouni et al., 1998). We recall the pertinent analysis concerning this criterion in this article for the sake of completeness and compare it with a similar criterion that we shall introduce for the rational approximation here.

Table 4
Contact: evaluation of $a_{ms}$[a]

| Order | | 10 | 15 | 20 | 25 | 30 |
|---|---|---|---|---|---|---|
| $\epsilon = 10^{-7}$ | $a_{ms}$ | 8.7918 | 11.3423 | 12.7486 | 13.6222 | 14.2121 |
| | $R_B(a_{ms}) \times 10^4$ | −1.0687 | −1.9982 | −2.9842 | −4.007 | −5.0571 |
| | $\log_{10}$(residual) | −5.04239 | −4.9313 | −4.8812 | −4.8534 | −4.8361 |
| $\epsilon = 10^{-5}$ | $a_{ms}$ | 14.6657 | 15.7610 | 16.2452 | 16.5036 | 16.6581 |
| | $R_B(a_{ms}) \times 10^3$ | −0.6223 | −1.2467 | −2.0757 | −3.1350 | −4.4532 |
| | $\log_{10}$(residual) | −2.8272 | −2.7986 | −2.7843 | −2.7655 | −2.7298 |
| $\epsilon = 10^{-3}$ | $a_{ms}$ | 24.4638 | 21.8999 | 20.7008 | 19.9946 | 19.5250 |
| | $R_B(a_{ms}) \times 10^4$ | 3.3161 | 4.5777 | 5.8192 | 7.0781 | 8.3798 |
| | $\log_{10}$(residual) | −0.6185 | −0.6770 | −0.7165 | −0.7373 | −0.7741 |

[a] In this case, the contact force $R_B$ at point B varies much more rapidly than the parameter $a$ near the end of step.

Formula (9) depends on two parameters, the truncation order $n$ and the accuracy parameter $\epsilon$. The order $n$ is generally chosen a priori with the aim to minimize the computation time. The values $n = 15$ or $n = 20$ often turn out to be optimal. Thus, the problem is to find an appropriate value of the accuracy parameter so as to ensure a sufficiently small value of the final residual vector. In Tables 3 and 4, we present the step length $a_{ms}$ and the final residual at the end of the step as a function of the index $n$ and the accuracy parameter. The step length increases significantly with the order, which explains the importance of a large number of terms. It also increases with the parameter, and in the two cases shown, one sees a strong relation between the parameter and the final value of the residual. For instance, in the case of the cylinder, a small value of $\epsilon$ ($\epsilon = 10^{-7}$) leads to a final residual of about $10^{-6}$, whatever the order and the same holds for the other results presented in Tables 3 and 4. So, for each problem, there seems to be an optimal value of ($\epsilon$). Unfortunately this optimal value depends on the problem under consideration. In what follows, we shall choose $\epsilon = 10^{-5}$ in the case of the cylinder and $\epsilon = 2.10^{-7}$ in the contact problem, to ensure a residual between $10^{-4}$ and $10^{-5}$, that eventually will lead to a residual of about $10^{-3}$ when several computational steps have been carried out.

The reduction of step length due to the strategy without correction can be estimated accurately: for instance, in the case of the cylinder and with the series, the ratio $a_{ms}/a_{LS}$ is 0.74 for $\epsilon = 10^{-7}$ (final residual $\epsilon = 10^{-6}$) and 0.79 to get a final residual equal to $\epsilon = 10^{-5}$ (Tables 1 and 3). Note that, in the contact case, it is dangerous to choose the parameter $\epsilon$ too large. Indeed, for $\epsilon = 10^{-3}$, a jump seems towards the physically non-existent branch of the hyperbolic regularized contact law that is determined by the wrong sign of the contact force.

The relation between the values of the accuracy parameter and the final residual, the comparison between the value of $a_{ms}$ and the radius of convergence, confirm the relevance and the efficiency of the criterion (9) for the end of step, whose reliability has already been proved by many applications to problems in various fields.

## 3. A continuation algorithm based on Padé approximants

We shall now establish a continuation algorithm based on the rational approximation (6), that is presented in details in Appendix A. It is essential to define a criterion that measures the range of validity of a rational representation. Generally, the residual error seems to increase monotonically inside this range of validity, as it does the truncated power series (Najah et al., 1998; Braikat et al., 1997). Nevertheless, it is not sufficient to check the values of the residual at only the end or at some distinct points of an interval $[0, a]$,

because of the possible occurrence of 'defects' in a rational approximation (Baker and Morris, 1996). Indeed, when dealing with Padé approximants, the numerator and the denominator of the fractions in Eq. (2) may have roots that are very closely spaced so that the actual function and its approximation are almost equal except in a very small part of the interval. This numerical phenomenon is called a defect of the rational approximation. As a computational code in engineering must be absolutely reliable, these defects must be eliminated from the expression of the solution path. To achieve this, we compute all the roots of the common denominator $D_n$ of the rational approximation (6) by using a Bairstow algorithm. This algorithm is reiterated in Appendix B. We designate by $r$, the smallest real root of $D_n$. If $r$ is smaller than the number $a_{\mathrm{ms}}$ defined by Eq. (9), we give up the rational representation and we go back to the series, at least for the current step. Generally, the smallest root $r$ will be larger than $a_{\mathrm{ms}}$. We now try to introduce a criterion for the value $a_{\mathrm{mp}}$ of the control parameter, which indicates when the Padé approximation (6) is not acceptable. This limit of validity will be sought in the interval $[a_{\mathrm{ms}}, r]$.

### 3.1. The criterion to define the step length

According to several trial computations that we conducted, the rational approximations for different orders of truncation yield results that are very close when the parameter $a$ is inside the domain of validity, but beyond this domain they diverge wildly. This is illustrated by Fig. 3, where several rational approximations are pictured for the problem of the cylindrical shell.

Thus, a simple way to achieve our goal seems to extend criterion (9) or (8) to the rational case. In this case, one has only to require that the difference between two rational solutions at consecutive orders remains small at the end of the step. The maximal value $a_{\mathrm{mp}}$ is then defined by

$$\frac{\|\mathbf{P}_n(a_{\mathrm{mp}}) - \mathbf{P}_{n-1}(a_{\mathrm{mp}})\|}{\|\mathbf{P}_n(a_{\mathrm{mp}}) - \mathbf{u}_0\|} \simeq \epsilon_2, \tag{10}$$

where $\epsilon_2$ is a small number. The number $a_{\mathrm{mp}}$ in the interval $[a_{\mathrm{ms}}, r]$ is then sought by the method of bisection using criterion (10). This criterion avoids the computation of many residual vectors, which would otherwise add to the volume of computations.

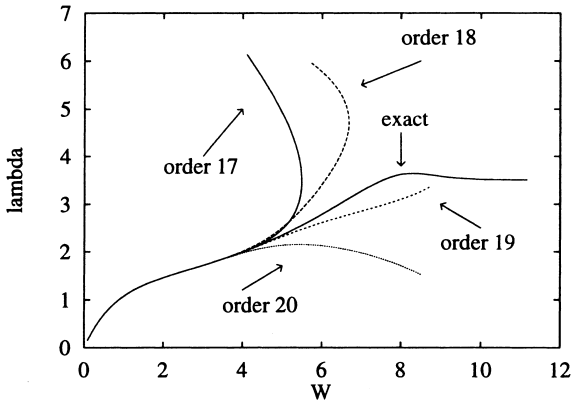


Fig. 3. Cylindrical shell: comparison between exact and Padé solution with different truncation orders. Loading parameter/radial displacement.

### 3.2. Some examples with $a_{mp}$ computation

We consider the two problems previously described concerning the buckling of cylindrical shell and the contact problem with a plane obstacle. The so-computed values of the step length: $a_{\mathrm{ms}}$ for the polynomial approximation and $a_{\mathrm{mp}}$ for the one based on Padé approximants are presented in Tables 5 and 6.

The accuracy parameters are chosen as $\epsilon_1 = 10^{-5}$, $\epsilon_2 = 10^{-5}$ ($\epsilon_2 = 2.10^{-7}$ in the contact problem) and we consider various truncation orders 10, 15, 20, 25. With these accuracy parameters, the solution obtained at the end of step is better than the rational approximation. Nevertheless, the Padé approximants increase the domain of validity. This improvement does not appear to be as important as in the contact case, but remember that the value of the contact force is more relevant than the path parameter to evaluate the part of the solution branch that has been accounted for.

Note that the Padé approximants are calculated by a simple Gram–Schmidt orthogonalization procedure (Appendix A) which adds only little in computing time as compared with the computation of the series.

#### 3.2.1. Other examples

In this example, we consider a curved shell hinged along two opposite sides, which is submitted to a concentrated force at the central point (Fig. 4). Assuming symmetry conditions, only one quarter of the shell is studied and discretized with 200 shell elements of DKT type.

The analysis is carried out with two different values of the thicknesses $h_1 = 6.35$ mm and $h_2 = 12.7$ mm. The truncation order has been fixed at 20. Figs. 5 and 6, describe the first solution step obtained by the series and the Padé approximants using accuracy parameters $\epsilon_1 = \epsilon_2 = 10^{-5}$.

With the thick shell, criterion (9) gives a limit value $a_{\mathrm{ms}} = 67.21$, which corresponds to a deflection $w = 12.04$ mm. With criterion (10), the range of validity of the Padé representation is approximately $a_{\mathrm{mp}} = 82.09$, which corresponds to $w = 13.83$ mm. The modulus of the first complex pole is $a_{\mathrm{rc}} = 88.52$.

Table 5
Cylinder: the quality of the series and of the Padé solution at the end of the first step with the two displacement criteria

| Order | Series | | Padé | |
|---|---|---|---|---|
| | $a_{\mathrm{ms}}$ | $\log_{10}$(residual) | $a_{\mathrm{mp}}$ | $\log_{10}$(residual) |
| 10 | 6.3302 | −4.0386 | 7.7173 | −4.0769 |
| 15 | 8.5670 | −3.9336 | 11.6327 | −4.2902 |
| 20 | 9.8623 | −3.8568 | 14.3456 | −3.8822 |
| 25 | 10.7049 | −3.7511 | 16.6730 | −4.2302 |
| 30 | 11.3021 | −3.6352 | 18.2748 | −4.6459 |

Table 6
Contact: the quality of the series and of the Padé solution at the end of the first step with the two displacement criteria. $R$ is the contact force at node B with $\eta = 10^{-4}$

| Order | Series | | | Padé | | |
|---|---|---|---|---|---|---|
| | $a_{\mathrm{ms}}$ | $R_{\mathrm{B}}(a_{\mathrm{ms}}) \times 10^3$ | $\log_{10}$(residual) | $a_{\mathrm{mp}}$ | $R_{\mathrm{B}}(a_{\mathrm{mp}}) \times 10^3$ | $\log_{10}$(residual) |
| 10 | 14.6657 | −0.6223 | −3.5793 | 14.9890 | −0.7365 | −5.3619 |
| 15 | 15.7610 | −1.2467 | −3.5438 | 16.0916 | −1.7163 | −5.3659 |
| 20 | 16.2452 | −2.0757 | −3.5297 | 16.4461 | −2.8018 | −5.4585 |
| 25 | 16.5036 | −3.1350 | −3.3079 | 16.5729 | −3.5819 | −5.3374 |
| 30 | 16.6581 | −4.4532 | −3.06284 | 16.7582 | −5.9054 | −4.5612 |

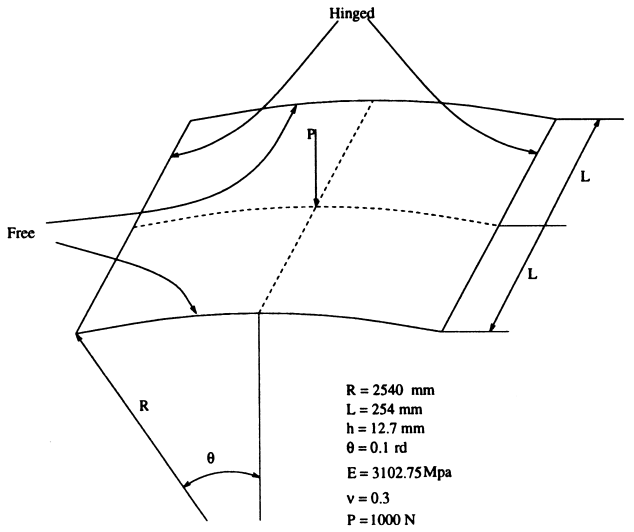


Fig. 4. Elastic cylindrical shell loaded by a concentrated force.

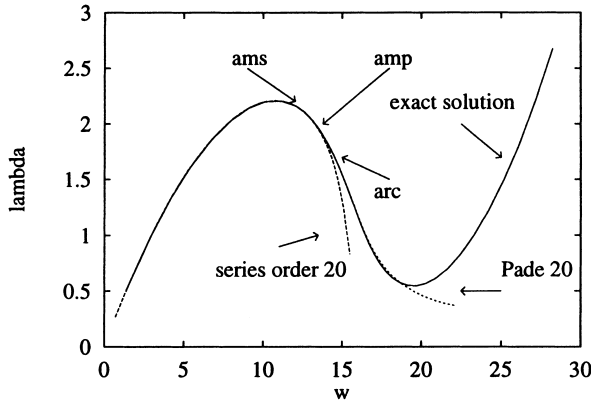


Fig. 5. Thick shell: loading parameter/displacement of the central point, validity limit of the polynomial and the rational solution.

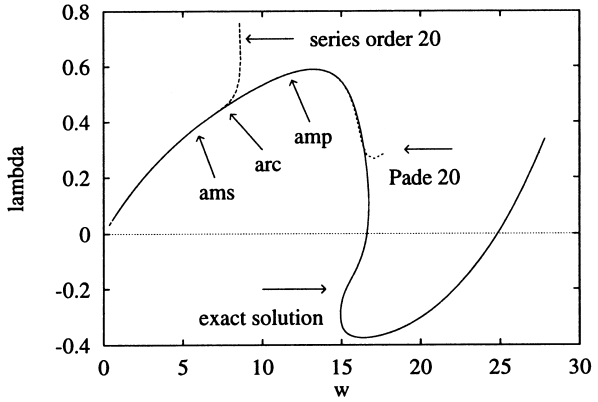


Fig. 6. Thin shell: loading parameter/displacement of the central point, validity limit of the polynomial and the rational solution.

Therefore, in this case the range of validity of the rational approximation does not extend to the radius of convergence.

The extension of the step length seems to be more important with the thin shell example. The validity bounds for the two representations are $a_{\mathrm{ms}} = 21.98$ and $a_{\mathrm{mp}} = 48.32$ corresponding to $w = 6.01$ and $w = 11.87$, respectively. The modulus of the first complex pole is $a_{\mathrm{rc}} = 30.14$, so that the range of validity of the rational approximation extends much beyond the radius of convergence.

### 3.3. Continuation algorithm

In this section, we propose the continuation algorithm based on the rational representation. It can be summarized as follows:

(1) Computation of the asymptotic solution:
   – Compute the series until a given order $n$.
   – Calculate the validity limit $a_{\mathrm{ms}}$ of the polynomial solution by the displacement criterion (9)
(2) Computation of the simultaneous Padé approximants (see Appendix A)
   – Gram–Schmidt orthogonalization procedure.
   – Computation of the denominator $D_{n-1}$.
(3) Choice of the solution:
   – Solving $D_{n-1} = 0$ by the Bairstow algorithm (see Appendix B), the first real root is designed by $r$.
   – If $|r| < |a_{\mathrm{ms}}|$, we consider the polynomial solution:

$$\begin{cases} \mathbf{S}_n(\mathbf{u}(a)), & a \in [0, a_{\mathrm{ms}}], \\ S_n(\lambda(a)). \end{cases}$$

   – If $|r| > |a_{\mathrm{ms}}|$, calculate $a_{\mathrm{mp}}$, satisfying criterion (10), in the interval $[a_{\mathrm{ms}}, r]$, and form the Padé approximant solution:

$$\begin{cases} \mathbf{P}_n(\mathbf{u}(a)), & a \in [0, a_{\mathrm{mp}}], \\ P_n(\lambda(a)). \end{cases}$$

(4) Redefine a new starting point for the next step which corresponds to the end of step obtained at (3) for $a = a_{\mathrm{ms}}$ or $a = a_{\mathrm{mp}}$ and go back to (1).

## 4. Applications of the continuation algorithm

In this section, we consider various numerical examples in order to discuss and validate the algorithm presented in Section 3: the previously described problems of the shallow shells under concentrated loads and the one of the cylindrical shell, the contact problem and the classical buckling problem of an arch involving two bifurcating branches. In all the cases, the series are truncated at the order 20. In these calculations, the total step number is the measure of efficiency of the algorithm and the rational approximation will be compared with the polynomial one and sometimes with classical iterative methods.

### 4.1. Shallow shells loaded by a concentrated force

First, we considered the two curved shell problems (Fig. 4), whose first computational step has just been analyzed and we applied the continuation methods till the deflection reaches the value $w = 30.5$ mm. With the rational approximation, this solution path requires only two steps for the thick shell and seven steps with the thin shell, whereas the same computation requires, respectively, four and 12 steps with using the

series expansion. So, it appears that the use of the Padé approximants leads to a reduction of the computational steps by a factor of about two.

These classical benchmarks had been previously considered in many articles, for instance, in Ammar (1996) and Simo et al. (1990). According to the first author, the most rapid iterative method is the modified Newton method, that yields the curve of Fig. 5 in 30 steps, i.e. 30 matrix decompositions, but as usually, the method is not reliable and diverges if one prescribes a larger step. As for the Newton–Raphson method, most of authors solve the thick shell problem in at least 10 steps and the thin one in at least 15 steps, with about three iterations per step. This results in 40–70 matrix decompositions in the first case, 60–100 in the second one. In terms of computation time, one can consider that one step with the ANM is equivalent to two matrix decompositions (Cochelin et al., 1994a; Zahrouni et al., 1999, 1998), so that the computation time within the present method is equivalent to four and 14 matrix decompositions within Newton–Raphson algorithms: this is an illustration of the efficiency of the presented continuation method, as compared with classical incremental-iterative algorithms. Remark also that it does not seem possible to describe the two response curves with less than 10 and 15 points: this type of requirement limits the efficiency of classical methods as much as problems of convergence.

### 4.2. Cylindrical shell

For the buckling problem of the cylindrical cell (Fig. 1), the number of steps is reduced from 9 with the series, to 5 with the new algorithm. The points at which a new computation of the series is made are shown in Fig. 7. The step length between these points varies along the response curve and this length is shorter in the neighborhood of the maximum load point but the step length of the method with the series expansion is generally smaller than the step length of the new procedure. Roughly speaking, the ratio of this gain is about 40% or 50% and this gain is more or less uniform in the present case, because the ratio $a_{\mathrm{mp}}/a_{\mathrm{ms}}$ varies in a small range from 0.35 to 0.70.

As expected, the residual increases along the solution path except in the beginning see step 2 in Table 7, but it remains reasonably small along the solution path (maximal value $10^{-2.8}$) so that the algorithm provides a satisfactory solution without any corrections. With the chosen accuracy parameters $\epsilon_1$ and $\epsilon_2$, we get about the same quality of solution (residual at the evaluation points remains between the bracket $10^{-4}$–$10^{-3}$) so that the presented comparison between rational and polynomial representations is significant.

Finally, please observe that the real poles are far outside the interval $[0, a_{\mathrm{mp}}]$ so that in this example, it was not necessary to introduce the procedure to eliminate the 'defects' of the rational representation.

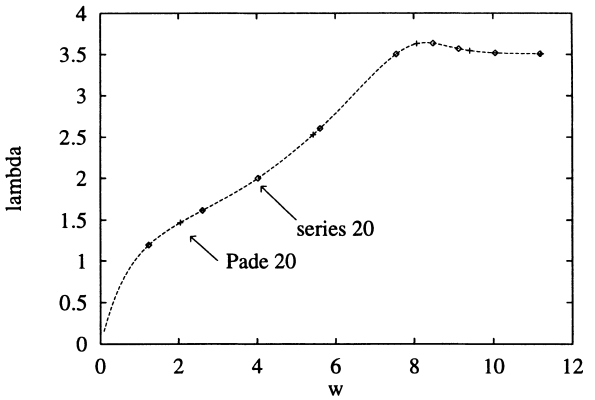


Fig. 7. Cylinder: polynomial and rational representation truncated at order 20. Loading parameter/radial displacement.

Table 7
Continuation algorithm with rational representation, $\epsilon_1 = \epsilon_2 = 10^{-5}$

| Step | $a_{ms}$ | $a_{mp}$ | First real pole | $\log_{10}$(residual) |
|---|---|---|---|---|
| 1 | 9.8623 | 14.3455 | 153.3270 | −3.8821 |
| 2 | 7.7721 | 22.0473 | 53.4529 | −3.9564 |
| 3 | 20.7197 | 29.4371 | 90.4589 | −2.9707 |
| 4 | 10.7401 | 22.7509 | 74.7979 | −2.8213 |
| 5 | −18.3048 | −26.4700 | −83.6267 | −2.8010 |

### 4.3. Buckling of a circular arch

We consider a deep circular arch submitted to a vertical force applied at the center and to a perturbation force $P = F/100$ placed excentrally (Fig. 8). To analyze this classical benchmark problem, we used the same software as in the previous examples, that is based on the DKT shell element, which is based on the framework of small moderate rotations. Of course, that framework is not perfectly adapted to the case of a deep shell but the equilibrium path (Fig. 9) has qualitatively the same features as the deep shell model. There are two quasi-bifurcations in this response curve: that is why this example is a severe test for the reliability of a path following technique. As this is a quasi-bifurcation problem, the computations cannot be

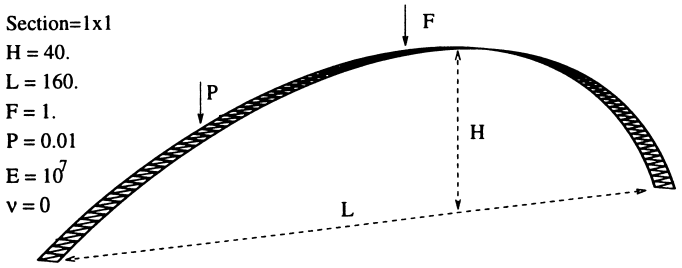


Fig. 8. Arch: 200 elements DKT mesh, 1212 dof.

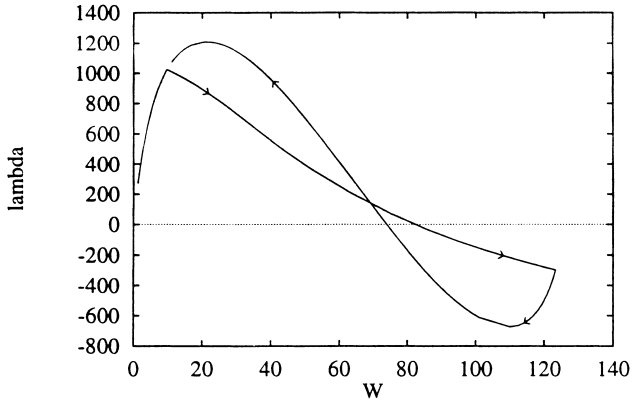


Fig. 9. Equilibrium path: loading parameter/displacement at the middle of the arch.

Table 8
Padé continuation algorithm with truncation at order 20: $\epsilon_1 = 10^{-14}$, $\epsilon_2 = 10^{-9}$

| Step | $a_{ms}$ | $a_{mp}$ | First real pole | $W$ | $\log_{10}$(Padé residual) |
|---|---|---|---|---|---|
| 1 | 496.7623 | 766.0646 | 1035.3670 | 5.3821 | −7.5602 |
| 2 | 190.5040 | 252.4374 | 261.2850 | 9.6583 | −8.0901 |
| 3 | 6.7843 | 8.8822 | 8.8843 | 9.8741 | −8.0967 |
| 4 | 0.001002 | 0.001512 | 0.00236 | 9.8742 | −8.0959 |
| 5 | 0.00113 | 0.00228 | 0.00296 | 9.9077 | −8.0952 |
| 10 | −0.6326 | −10.2266 | −62.0343 | 10.0243 | −6.2804 |
| 11 | −12.3055 | – | −9.0793 | 37.5081 | −6.2799 |
| 15 | −112.5832 | −313.3450 | −380.2656 | 123.3377 | −5.7953 |
| 20 | −16.1427 | −27.0950 | −31.3806 | 122.4159 | −4.9616 |
| 25 | −2.6802 | −66.2319 | −511.0942 | 88.7651 | −4.7605 |
| 30 | 87.8300 | 216.1468 | 2140.8985 | 22.5629 | −4.6465 |
| 39 | −46.8303 | −73.7248 | −89.8615 | 10.2850 | −5.0552 |

carried out without choosing very small values for the accuracy parameters ($\epsilon_1 = 10^{-14}$ and $\epsilon_2 = 10^{-9}$). As a consequence, the residual remains very small along the computed path and no iterative corrections are needed. With the series representation, 200 solution steps are necessary to obtain the solution path, which reduces to 39 with the Padé representation. These large numbers of steps are due to the large curvature of the path close to the bifurcation points: for instance, one is close to the first bifurcation point from step 2 to step 10, to the second one from step 15 to step 20 and again close to the first one from steps 30 to 39 (Table 8). As in the previous example, the ratio $a_{ms}/a_{mp}$ is generally in the range 0.35–0.75 so that the rational approximation should reduce the number of steps by a factor of about two. In actual run, the number of steps is reduced by a factor of five, which is due to very large ratios $a_{mp}/a_{ms}$ for a few steps (steps 10 and 25).

In one case (step 11), we found a real pole in the interval $[0, a_{ms}]$, and according to the algorithm, the 11th step is carried out with the series representation. This establishes that the computation of the poles is effective and improves the robustness of the algorithm. In another case (step 3), the step length $a_{mp}$ and the smallest real pole lie very close together, what implies that one can get a very accurate solution up to the pole: this phenomenon is typical of a 'defect' in a Padé approximant and it shows that it is not sufficient to check only some values of the residual in order to ensure the resolution of the solution path in a given interval.

This example shows that the Padé algorithm combines efficiency and robustness. Indeed, it reduced the number of steps with respect to the series with a factor of five and it permitted to compute this intricate equilibrium path without any difficulty. The analysis also shows the importance of the control of the poles of the rational representation in the formulation of the algorithm.

This example has been designed to be a severe test for a path following technique, especially the smallness of the force ratio $P/F$. We have tried to achieve this computation by the standard algorithms of the commercial code ABAQUS, but the algorithms have diverged. Likely the most efficient would be to apply a procedure specific for bifurcation problems, see for instance, Vannucci et al. (1998), but here the aim is to discuss generic path following technique.

### 4.4. Contact between a 2-D elastic beam and a plane rigid surface

We now return to the contact previously described (Fig. 2). The accuracy parameters are chosen as given in Table 9 together with the particulars of the computation. To obtain the solution path up to $\lambda = 1, 90$ steps are needed with the series expansion but only 51 steps with the rational representation. Compared to this result the engineering code (ABAQUS) requires the factoring of 128 stiffness matrices. The residuals in

Table 9
Padé continuation algorithm with truncature at order 20: $\epsilon_1 = 10^{-5},\ \epsilon_2 = 2.10^{-7}$

| Step | $a_{ms}$ | $a_{mp}$ | $a_{mp}/a_{ms}$ | First real pole | $\log_{10}$(Padé residual) |
|---|---|---|---|---|---|
| 1 | 16.2451 | 16.4461 | 1.01 | 17.0490 | −5.6355 |
| 2 | 0.552861 | 0.552869 | 1.00 | 0.6789 | −4.5939 |
| 3 | 0.0950 | 0.1410 | 1.48 | 0.1563 | −4.6296 |
| 4 | 0.1364 | 0.25537140 | 1.87 | 0.255385 | −4.6223 |
| 5 | 0.3106 | 2.0742 | 6.67 | 5.0135 | −4.2449 |
| 10 | 0.1753 | 0.2435 | 1.38 | 2.3579 | −3.9892 |
| 15 | 0.1125 | 0.1499 | 1.33 | 0.1624 | −3.5283 |
| 20 | 0.0650 | 0.1495 | 2.29 | 0.4028 | −3.0608 |
| 25 | 0.0421 | 0.1461 | 3.46 | 0.3193 | −2.9851 |
| 30 | 0.0983 | 0.1153 | 1.17 | 277.8555 | −2.7010 |
| 32 | 0.1054 | – | – | 0.06634 | −2.4639 |
| 35 | 0.0901 | 0.1163 | 1.29 | 0.2995 | −2.5477 |
| 40 | 0.0129 | 0.0206 | 1.58 | 0.0206 | −2.6758 |
| 45 | 0.01003 | 0.0158 | 1.57 | 0.01619 | −2.8206 |
| 51 | 0.0733 | 0.2538 | 3.46 | 0.7953 | −3.1915 |

our procedure remain relatively small although we could have obtained a high accuracy if we had introduced some corrector iterations after step 25. As in the previous case, some of the steps (5, 25, 51) seem to have played an important part in the improvement of the calculation by the rational approximation. In at least four cases, the necessity to control the poles of the rational approximation is manifest: in step 32, where a real pole is detected in the range of validity of the series and in step 4, 40 and 45, where the step length $a_{mp}$ is almost equal to the first real pole.

## 5. Conclusion

In this article, we proposed a new variant of a continuation algorithm based on Padé approximants and demonstrated the efficiency and the robustness of the method. Roughly speaking, the method is capable to reduce the number of steps by a factor of two as compared to the same method based on series expansion; in one case this fact was even five. In principle, the rational representation is less stable than the polynomial one. That is why, as a precaution, we introduced a new step length criterion. The numerical tests that we carried out show that this criterion cannot be omitted. As far as the reliability of the algorithm is concerned, it never failed in the five examples that we studied here inspite of the fact that these examples involve limit points, quasi-bifurcations and unilateral contact.

Incidentally, the expectation that the knowledge of the poles permits one to estimate the radii of convergence of the series is confirmed by these calculations.

According to several recent studies (Ammar, 1996; Cochelin, 1994; Cadou et al., 1998; Zahrouni et al., 1999), the representation by series leads to continuation method, which is more efficient than the classical incremental-iterative method. The method that we proposed here can reduce by half the computational time with respect to the series method. It is likely that the present method is not really the best possible variant in the class of asymptotic numerical algorithms because, we considered only a type of Padé approximant among the many possibilities (Baker and Morris, 1996; Brezinski and Iseghem, 1994) that exist. The reduced basis algorithms (Lewandowski, 1987; Noor, 1981; Noor and Peters, 1980, 1981) could also be modified with a view to diminish their computational time.

**Acknowledgements**

This article is dedicated to Prof. W.T. Koiter, who was the author of many decisive contributions in various fields. In elastic stability, he was 20 years ahead of the engineering community and 25 years ahead of the mathematicians working on bifurcation theory. One of us (Michel Potier-Ferry) has often interacted with him and keeps a delightfull memory of his simplicity and his sharp scientific views.

## Appendix A. Padé approximants for series of vector

Since H. Padé's Thesis, 1892, we know that rational fractions are more appropriate than polynomials to represent a function. One can find a modern presentation of Padé approximant in Baker and Morris (1996). We use Padé approximants in the ANM in the following manner:

(1) From the vectors $\mathbf{U}_1, \mathbf{U}_2, \ldots, \mathbf{U}_p$, we build up an orthogonal basis by the classical Gram–Schmidt procedure (We detail the computations for $p = 6$):

$$\begin{cases} \mathbf{U}_1 = \alpha_{11}\mathbf{U}_1^*, \\ \mathbf{U}_2 = \alpha_{21}\mathbf{U}_1^* + \alpha_{22}\mathbf{U}_2^*, \\ \mathbf{U}_3 = \alpha_{31}\mathbf{U}_1^* + \alpha_{32}\mathbf{U}_2^* + \alpha_{33}\mathbf{U}_3^*, \\ \mathbf{U}_4 = \alpha_{41}\mathbf{U}_1^* + \alpha_{42}\mathbf{U}_2^* + \alpha_{43}\mathbf{U}_3^* + \alpha_{44}\mathbf{U}_4^*, \\ \mathbf{U}_5 = \alpha_{51}\mathbf{U}_1^* + \alpha_{52}\mathbf{U}_2^* + \alpha_{53}\mathbf{U}_3^* + \alpha_{54}\mathbf{U}_4^* + \alpha_{55}\mathbf{U}_5^*, \\ \mathbf{U}_6 = \alpha_{61}\mathbf{U}_1^* + \alpha_{62}\mathbf{U}_2^* + \alpha_{63}\mathbf{U}_3^* + \alpha_{64}\mathbf{U}_4^* + \alpha_{65}\mathbf{U}_6^* + \alpha_{66}\mathbf{U}_6^*. \end{cases}$$

Then, we introduce this into the polynomial representation, which introduces six polynomials with a decreasing degree (from 5 to 0) as factors of the vector fields $\mathbf{U}_k$

$$\begin{aligned} \mathbf{U} - \mathbf{U}_0 = {} & a\mathbf{U}_1^*(\alpha_{11} + a\alpha_{21} + a^2\alpha_{31} + a^3\alpha_{41} + a^4\alpha_{51} + a^5\alpha_{61}) + a^2\mathbf{U}_2^*(\alpha_{22} + a\alpha_{32} + a^2\alpha_{42} + a^3\alpha_{52} + a^4\alpha_{62}) \\ & + a^3\mathbf{U}_3^*(\alpha_{33} + a\alpha_{43} + a^2\alpha_{53} + a^3\alpha_{63}) + a^4\mathbf{U}_4^*(\alpha_{44} + a\alpha_{54} + a^2\alpha_{64}) + a^5\mathbf{U}_5^*(\alpha_{55} + a\alpha_{65}) \\ & + a^6\mathbf{U}_6^*(\alpha_{66}). \end{aligned}$$

(2) We replace the polynomials by Padé approximants having the same denominator ($D_5 = d_1 + ad_2 + \cdots + a^5 d_5$), in the following way:

$$\begin{cases} \alpha_{11} + a\alpha_{21} + a^2\alpha_{31} + a^3\alpha_{41} + a^4\alpha_{51} + a^5\alpha_{61} \approx \frac{b_0 + ab_1 + a^2b_2 + a^3b_3 + a^4b_4}{D_5}, \\ \alpha_{22} + a\alpha_{32} + a^2\alpha_{42} + a^3\alpha_{52} + a^4\alpha_{62} \approx \frac{c_0 + ac_1 + a^2c_2 + a^3c_3}{D_5}, \\ \alpha_{33} + a\alpha_{43} + a^2\alpha_{53} + a^3\alpha_{63} \approx \frac{e_0 + ae_1 + a^2e_2}{D_5}, \\ \alpha_{44} + a\alpha_{54} + a^2\alpha_{64} \approx \frac{f_0 + af_1}{D_5}, \\ \alpha_{55} + a\alpha_{65} \approx \frac{g_0}{D_5}. \end{cases}$$

The coefficients $b_i$, $c_i$, $e_i$, $f_i$ and $g_i$ are computed by the same principles as with the classical Padé approximants; we require that each fraction has the same Taylor expansions as the corresponding polynomials up to order 5, 4, 3, 2, 1, respectively. This results:

$$\begin{aligned} b_0 &= \alpha_{11}, \\ b_1 &= \alpha_{21} + \alpha_{11}d_1, \\ b_2 &= \alpha_{31} + \alpha_{21}d_1 + \alpha_{11}d_2, \\ b_3 &= \alpha_{41} + \alpha_{31}d_1 + \alpha_{21}d_2 + \alpha_{11}d_3, \\ b_4 &= \alpha_{51} + \alpha_{41}d_1 + \alpha_{31}d_2 + \alpha_{21}d_3 + \alpha_{11}d_4, \end{aligned}$$

$$
\begin{aligned}
c_0 &= \alpha_{22}, & e_1 &= \alpha_{43} + \alpha_{33}d_1,\\
c_1 &= \alpha_{32} + \alpha_{22}d_1, & e_2 &= \alpha_{53} + \alpha_{43}d_1 + \alpha_{33}d_2,\\
c_2 &= \alpha_{42} + \alpha_{32}d_1 + \alpha_{22}d_2, & f_0 &= \alpha_{44},\\
c_3 &= \alpha_{52} + \alpha_{42}d_1 + \alpha_{32}d_2 + \alpha_{22}d_3, & f_1 &= \alpha_{54} + \alpha_{44}d_1,\\
e_0 &= \alpha_{33}, & g_0 &= \alpha_{55},
\end{aligned}
$$

and the coefficients of $D_5 = d_1 + ad_2 + \cdots + a^5 d_5$ are solutions of the triangular system

$$
\begin{cases}
\alpha_{61} + \alpha_{51}d_1 + \alpha_{41}d_2 + \alpha_{31}d_3 + \alpha_{21}d_4 + \alpha_{11}d_5 = 0,\\
\alpha_{62} + \alpha_{52}d_1 + \alpha_{42}d_2 + \alpha_{32}d_3 + \alpha_{22}d_4 = 0,\\
\alpha_{63} + \alpha_{53}d_1 + \alpha_{43}d_2 + \alpha_{33}d_3 = 0,\\
\alpha_{64} + \alpha_{54}d_1 + \alpha_{44}d_2 = 0,\\
\alpha_{65} + \alpha_{55}d_1 = 0.
\end{cases}
$$

(3) After some rearrangements, we arrive at a new form of the previous rational representation, that involves only vectors $\mathbf{U}_k$ and the coefficients $d_i$

$$
\mathbf{U} - \mathbf{U}_0 = a\frac{D_4}{D_5}\mathbf{U}_1 + a^2\frac{D_3}{D_5}\mathbf{U}_2 + a^3\frac{D_2}{D_5}\mathbf{U}_3 + a^4\frac{D_1}{D_5}\mathbf{U}_4 + a^5\frac{1}{D_5}\mathbf{U}_5.
$$

We do the same for the control parameter

$$
\lambda - \lambda_0 = a\frac{D_4}{D_5}\lambda_1 + a^2\frac{D_3}{D_5}\lambda_2 + a^3\frac{D_2}{D_5}\lambda_3 + a^4\frac{D_1}{D_5}\lambda_4 + a^5\frac{1}{D_5}\lambda_5.
$$

## Appendix B. Bairstow's algorithm

The principle of this technique is to compute, two by two, the roots of a polynomial $D_n(a) = 0$ $(n \geqslant 2)$. The algorithm is described in what follows:

(1) As $D_n(a)$ admits at least two real or complex roots, it can be written as a product of a polynomial $Q(a)$ and a polynomial of second degree $a^2 - sa + p$, where $s$ and $p$ are, respectively the sum and the product of the two of roots.

The Euclidian division of $P_n(a)$ by $(a^2 - sa + p)$ leads to the equation:

$$
D_n(a) = (a^2 - sa + p)Q(a) + R(a), \tag{B.1}
$$

where

$$
\begin{cases}
Q(a) = q_n a^{n-2} + q_{n-1}a^{n-3} + \cdots + q_3 a + q_2,\\
R(a) = q_1 a + q_0.
\end{cases}
$$

The coefficients $q_1$ and $q_0$ depend on $s$ and $p$. The sought values of $s$ and $p$ are the values producing a zero of the polynomial $R(a)$. $s$ and $p$ are then solutions of the following non-linear system:

$$
\begin{cases}
q_0(s,p) = 0,\\
q_1(s,p) = 0.
\end{cases} \tag{B.2}
$$

Coefficients of the polynomials $Q$ and $R$ are obtained by identifying the powers of $(a)$ in Eq. (B.1):

Table 10
Cylinder: the loading parameter and the quality of the polynomial approximation, truncated at order 20, with respect to the parameter $a$

| $a/a_{rc}$ ($a_{rc} = 14.1$) | $\lambda$ | $\log_{10}$(residual) |
|---|---|---|
| 0.1006 | 0.2179 | −11.9749 |
| 0.2012 | 0.4223 | −11.9303 |
| 0.3018 | 0.6122 | −11.3110 |
| 0.4023 | 0.7862 | −8.7807 |
| 0.5030 | 0.9431 | −6.8014 |
| 0.6035 | 1.0820 | −5.1758 |
| 0.7041 | 1.2030 | −3.7950 |
| 0.7644 | 1.2674 | −3.0559 |
| 0.8047 | 1.3075 | −2.5944 |
| 0.9052 | 1.3997 | −1.5341 |
| 1.0059 | 1.4940 | −0.5904 |

Table 11
Cylinder: the loading parameter and the quality of the rational approximation, truncated at order 20, with respect to the parameter $a$

| $a/a_{rc}$ ($a_{rc} = 14.1$) | $\lambda$ | $\log_{10}$(residual) |
|---|---|---|
| 0.1622 | 0.3448 | −11.9435 |
| 0.3245 | 0.6529 | −11.9087 |
| 0.4867 | 0.9190 | −10.8543 |
| 0.6489 | 1.1388 | −8.0757 |
| 0.8112 | 1.3135 | −5.9032 |
| 0.9734 | 1.4525 | −4.2451 |
| 1.1357 | 1.5703 | −3.0547 |
| 1.2980 | 1.6786 | −2.2313 |
| 1.4601 | 1.7842 | −1.6580 |
| 1.6223 | 1.8907 | −1.2360 |

Table 12
Contact: the contact force, the clearance $h$ and the quality of the polynomial approximation, truncated at order 20, with respect to the parameter $a$

| $a/a_{rc}$ ($a_{rc} = 17.06$) | $R_B \times 10^3$ | $h_B$ | $\log_{10}$(residual) |
|---|---|---|---|
| 0.1370 | −0.0159 | 1.7253 | −9.9236 |
| 0.2739 | −0.0379 | 1.4507 | −9.8789 |
| 0.4109 | −0.0701 | 1.1761 | −9.8173 |
| 0.5478 | −0.1218 | 0.9015 | −7.5735 |
| 0.6848 | −0.2189 | 0.6270 | −5.6373 |
| 0.8217 | −0.4672 | 0.3526 | −4.0576 |
| 0.9176 | −1.1434 | 0.1608 | −3.1046 |
| 0.9587 | −2.4390 | 0.0788 | −2.7229 |
| 0.9724 | −3.7854 | 0.0514 | −2.5877 |
| 0.9861 | −8.1696 | 0.0241 | −2.3858 |

$$\begin{cases} q_n = d_n, \\ q_{n-1} = d_{n-1} + sq_n, \\ q_k = d_k + sq_{k+1} - pq_{k+2}, \quad 1 \leqslant k \leqslant (n-2), \\ q_0 = d_0 - pq_2. \end{cases} \tag{B.3}$$

By calculating the derivative (B.3) with respect to $s$ and $p$, we obtain the following equations:

$$\begin{cases} \frac{\partial q_n}{\partial s} = 0, \\ \frac{\partial q_{n-1}}{\partial s} = q_n, \\ \frac{\partial q_k}{\partial s} = q_{k+1} + s\frac{\partial q_{k+1}}{\partial s} - p\frac{\partial q_{k+2}}{\partial s}, \quad 1 \leqslant k \leqslant (n-2), \\ \frac{\partial q_0}{\partial s} = -p\frac{\partial q_2}{\partial s}. \end{cases}$$

$$\begin{cases} \frac{\partial q_n}{\partial p} = 0, \\ \frac{\partial q_{n-1}}{\partial p} = s\frac{\partial q_n}{\partial p}, \\ \frac{\partial q_k}{\partial s} = s\frac{\partial q_{k+1}}{\partial p} - q_{k+2} - p\frac{\partial q_{k+2}}{\partial p}, \quad 1 \leqslant k \leqslant (n-2), \\ \frac{\partial q_0}{\partial p} = -q_2 - p\frac{\partial q_2}{\partial p}. \end{cases}$$

(2) We get the values of $s$ and $p$ by applying an iterative Newton method to the system (B.2).

(3) We deduce the coefficients of the polynomial $Q(a)$, and go back to step (1) as long as necessary to calculate all the roots.

## Appendix C

For the sake of completeness, we present in detail the evolution of the residual along a step in typical cases discussed in Section 2. By comparison of Tables 10 and 11, it appears that the rational approximation improves the quality of the solution along the whole step. According to these tables, the requirement of a residual of $10^{-5}$ instead of $10^{-3}$ induces a small shortening of the step of about 20% or 30%: this illustrates the interest of a strategy without correction (Table 12).

## References

Almroth, B.O., Brogan, F.A., Stern, P., 1978. Automatic choice of global shape functions in structural analysis. AIAA 16, 525–528.

Ammar, S., 1996. Méthode asymptotique numérique perturbée appliquée à la résolution des problèmes non linéaires en grande rotation et grand déplacement. Thesis, Université Laval Québec, Faculté des sciences et de génie.

Azrar, L., Cochelin, B., Damil, N., Potier-Ferry, M., 1992. An asymptotic-numerical method to compute bifurcating branches. In: Ladvéze, P., Zienkiewicz, O.C. (Eds.), New Advances in Computational Structural Mechanics. Elsevier, Amsterdam, pp. 117–131.

Baker, G.A., Morris, P.G., Basic Theory, Encyclopedia of Mathematics and its Applications, vol. 13 1996 Addison-Wesley New York.

Boutyour, E.H., Cochelin, B., Potier-Ferry, M., 1993. Calcul des points de bifurcation par une méthode asymptotique numérique. I Congrès National de Mécanique au Maroc, pp. 371–378.

Braikat, B., Damil, N., Potier-Ferry, M., 1997. Méthode asymptotique numérique pour la plasticité. Revue Européenne des Éléments Finis 6 (3), 337–357.

Brezinski, C., Iseghem, V., 1994. Padé approximants. In: Ciarlet, P.G., Lions, J.L. (Eds.), Handbook of Numerical Analysis, vol. 3. North-Holland, Amsterdam.

Brunelot, J., 1999. Simulation de la mise en forme à chaud par la méthode asymptotique numérique. Thesis, Université de Metz.

Cadou, J.M., Cochelin, B., Damil, N., Potier-Ferry, M., 2000. Asymptotic numerical method for strongly non-linear problems: application to stationary Navier–Stokes equation and Petrov–Galerkin formulation. International Journal for Numerical Methods in Engineering, submitted for publication.

Cochelin, B., 1994. A path-following technique via an asymptotic-numerical method. Computers and Structures 53 (5), 1181–1192.

Cochelin, B., Damil, N., Potier-Ferry, M., 1994a. The asymptotic-numerical method: an efficient perturbation technique for non-linear structural mechanics. Revue Européenne des Eléments Finis 3 (2), 281–297.

Cochelin, B., Damil, N., Potier-Ferry, M., 1994b. Asymptotic numerical methods and Padé approximants for non linear elastic structures. International Journal for Numerical Methods in Engineering 37, 1187–1213.

de Boer, H., van Keulen, F., 1997. Padé approximants applied to a non-linear finite element solution strategy. Communications in Numerical Methods in Engineering 13, 593–602.

Elhage-Hussein, A., 1998. Modélisation des problèmes de contact par une méthode asymptotique numérique. Thesis, Université de Metz.

Elhage-Hussein, A., Damil, N., Potier-Ferry, M., 1998. An asymptotic numerical algorithm for frictionless contact problems. Revue Européenne des Éléments Finis 7 (1–3), 119–130.

Kawahara, M., Yoshimura, N., Nakagawa, K., Ohsaka, H., 1976. Steady and unsteady finite element analysis of incompressible viscous fluid. International Journal for Numerical Methods in Engineering 10, 437–456.

Lewandowski, R., 1987. Application of the Ritz method to the analysis of non-linear free vibrations of beams. Journal of Sound and Vibration 114 (1), 91–101.

Najah, A., Cochelin, B., Damil, N., Potier-Ferry, M., 1998. A critical review of asymptotic numerical methods. Archives of Computational Methods in Engineering 5 (1), 31–50.

Noor, A.K., 1981. Recent advances in reduction methods for non-linear problems. Computers and Structures 13, 31–44.

Noor, A.K., Peters, J.M., 1980. Reduced basis technique for non-linear analysis of structures. AIAA Journal 18 (4) 79–0747R, 1980.

Noor, A.K., Peters, J.M., 1981. Tracing post-limit-point paths with reduced basis technique. Computer Methods in Applied Mechanics and Engineering 28, 217–240.

Padé, H., 1892. Sur la représentation approachée d'une fonction par des fractions rationnelles. Annales de l'Ecole Normale Sup. 9 (3), 3–93.

Potier-Ferry, M., Cao, H.L., Brunelot, J., Damil, N., 2000. An asymptotic numerical method for numerical analysis of large deformation viscoplastic problems. Computers and Structures, in press.

Potier-Ferry, M., Damil, N., Braikat, B., Brunelot, J., Cadou, J.M., Cao, H., Elhage-Hussein, A., 1997. Traitement des fortes non-linéarités par la méthode asymptotique numérique. Comptes Rendus de l'Académie des Sciences t. 324 serie IIb, 171–177.

Simo, J.C., Fox, D.D., Rifai, M.S., 1990. On a stress resultant geometrically exact shell model, part III: computational aspects of the non-linear theory. Computer Methods in Applied Mechanics and Engineering 79, 21–70.

Thompson, J.M.T., Walker, A.C., 1968. The non-linear perturbation analysis of discrete structural systems. International Journal of Solids and Structures 4, 757–768.

Tri, A., Cochelin, B., Potier-Ferry, M., 1996. Résolution des équations de Navier–Stokes et détection des bifurcations stationnaires par une méthode asymptotique numérique. Revue Européenne des Éléments Finis 5 (4), 415–442.

Van-Dyke, M., 1984. Computed-extended series. Annual Review in Fluid Mechanics 16, 287–309.

Vannucci, P., Cochelin, B., Damil, N., Potier-Ferry, M., 1998. An asymptotic numerical method to compute bifurcating branches. International Journal for Numerical Methods in Engineering 41, 1365–1389.

Zahrouni, H., 1998. Méthode asymptotique numérique pour les coques en grandes rotations. Thesis, Université de Metz.

Zahrouni, H., Cochelin, B., Potier-Ferry, M., 1999. Computing finite rotations of shells by an asymptotic-numerical method. Computer Methods in Applied Mechanics and Engineering, 175, 71–85.

Zahrouni, H., Potier-Ferry, M., Elasmar, H., Damil, N., 1998. Asymptotic numerical method for non-linear constitutive laws. Revue Européenne des Éléments Finis, 7, 841–869.